PCCP

Accepted Manuscript

This is an *Accepted Manuscript*, which has been through the Royal Society of Chemistry peer review process and has been accepted for publication.

Accepted Manuscripts are published online shortly after acceptance, before technical editing, formatting and proof reading. Using this free service, authors can make their results available to the community, in citable form, before we publish the edited article. We will replace this *Accepted Manuscript* with the edited and formatted *Advance Article* as soon as it is available.

You can find more information about *Accepted Manuscripts* in the **Information for Authors**.

Please note that technical editing may introduce minor changes to the text and/or graphics, which may alter content. The journal's standard **Terms & Conditions** and the **Ethical guidelines** still apply. In no event shall the Royal Society of Chemistry be held responsible for any errors or omissions in this *Accepted Manuscript* or any consequences arising from the use of any information it contains.

ARTICLE TYPE

Impact of Electrode Potential and Solvent on the Electroreduction of CO_2: A Comparison of Theoretical Approaches[†‡]

Stephan N. Steinmann,[a] **Carine Michel,**[a,b]**, Renate Schwiedernoch,**[c] **and Philippe Sautet**[a,b*]

Since CO_2 is a readily available feedstock throughout the world, the utilization of CO_2 as a C1 building block for the synthesis of valuable chemicals is a highly attractive concept. However, due to its very nature of energy depleted "carbon sink", CO_2 has a very low reactivity. Electrocatalysis offers the most attractive means to activate CO_2 through reduction: the electron is the "cleanest" reducing agent whose energy can be tuned to the thermodynamic optimum. In protic conditions, the reduction of CO_2 over many metal electrodes results in formic acid. Thus, to open the road to its utilization as a C1 building block, the presence of water should be avoided to allow a more diverse chemistry, in particular for C–C bond formation with alkenes. In those conditions, the intrinsic reactivity of CO_2 can generate carbonates and oxalates by C–O and C–C bond formation, respectively. On Ni(111), almost exclusively carbonates and carbon monoxide are evidenced experimentally. Despite recent progress in modelling electrocatalytic reactions, determining the actual mechanism and selectivities between competing reaction pathways is still not straight forward. At the simple but important example of the intrinsic reactivity of CO_2 under aprotic conditions, we highlight the shortcomings of the popular linear free energy relationship for electrode potentials (LFER-EP). Going beyond this zeroth order approximation by charging the surface and thus explicitly including the electrochemical potential into the electronic structure computations, allows to access more detailed insights, shedding light on coverage effects and on the influence of counterions.

1 Introduction

Heterogeneous electrocatalysis is at the heart of advanced energy technologies such as hydrogen production[1] and fuelcells.[2] Furthermore, electrochemistry, in combination with photovoltaic cells, promises access to "green" and "mild" redox chemistry.[3–5] In particular, the electroreduction of CO_2 is a conceptually attractive avenue: electrochemistry activates the intrinsically rather inert green-house gas under mild conditions (i.e., low pressure and temperature), enabling to utilize CO_2 as a C1 building block in C–C coupling reactions[6–9] or to generate small, energy rich molecules such as CO, methanol or formic acid.[10–13]

In protic media, the reduction of CO_2 competes with H_2 evolution and mixtures of CO + H_2O, formic acid and very small amounts of hydrocarbons are observed in general.[14,15] Hence, the efficient use of CO_2 as a C1 building block precludes the presence of water and protons. For instance the electroreduction of CO_2 in DMF in the presence of a diene over Ni has been reported to yield C–C coupled products, in particular the dicarboxylates.[6,7,16–18] However, the existing procedure is not very efficient in terms of yield and selectivity and the mechanism is poorly understood. In addition, in aprotic solutions, CO_2 has an intrinsic reactivity, potentially yielding oxalate and a combination of CO and carbonate,[11,19] opening additional reaction paths.

Electrocatalysis is carried out in a complex environment, i.e., an electrolyte is required to increase the conductivity of the solution and the interface between the catalyst and the solvent is thin compared to the solution, making experimental characterization challenging.[20–25] Despite considerable efforts, we lack therefore detailed mechanistic understanding at the atomic level, hampering the rational design of novel catalysts. For all these reasons, research and development have still huge challenges to overcome in order to efficiently use CO_2 as a C1 building block.

Atomic scale modelling is a powerful tool to complement the experimental effort and provide detailed information under very well controlled conditions (catalyst surface, applied potential). However, computations are usually performed on simplified models and the influences of the electrolyte and of the solvent on the catalyst interfacial properties are rarely considered,[26] although their importance is well known from more empirical approaches.[27,28] The classical description of electrochemical systems typically relies on "empirical" or at least drastically simplified equations[29] (e.g., Marcus-Hush for electron transfer, Gouy-Chapman for the double layer properties or the Fokker-Planck equation for mass transport). These mesoscopic equations require system averaged parameters which can either be obtained by fitting to experiment or approximately extracted from first principles data. Although such multi-scale models[30,31] may correctly describe the relevant physics, the fundamental issue is that the central ingredient in electrocatalysis, the electrochemical potential, is far from being straight forward to include explicitly in a first principles approach at the atomic level.

The present study investigates the electroreduction of CO_2 in an aprotic solvent as a prerequisite for further investigations of the CO_2 coupling with alkenes.[6,7,16–18] Oxalate is the major product of CO_2 electrolysis under aprotic conditions on "inert" electrodes, in particular over Pb.[32,33] The proposed reaction mechanism, which is in good agreement with the high overpotentials required for this reaction, goes through $CO_2^{.-}$. The radical anion is supposed to be slightly stabilized by the surface at potentials below -1.8 V (vs. Ag/AgCl) and then undergo a fast surface assisted coupling.[34] On more reactive electrodes, and in particular over nickel, CO formation is frequently reported.[11,14]

The large majority of simulations of heterogeneous electrocatalysis rely on a simple model proposed in the seminal work by Norskov and coworkers under the name of the computational hydrogen electrode (CHE),[35] and its extension to other cations than H^+, e.g., Li^+[36] or Na^+, which we call linear free energy relationship for electrode potentials (LFER-EP). In this model, the electrochemical potential is assumed to affect only the chemical potential of the exchanged electrons and solvent effects are generally neglected. In a nutshell, this approach is an *a posteriori* correction of first principles studies of neutral metal surfaces in vacuum that are routine computations for some decades.[37] The CHE model leads to highly exploitable results,[38–44] despite its known limitations: absence of polarisation of adsorbed molecules and electron transfer strictly coupled to cation transfer. This implies, for example, that this method cannot grasp the transient anionic species $CO_2^{.-}$.

The comparison by Rossmeisl *et al.*[45] of the zeroth order approach CHE and the more advanced surface charge (SC) method of Filhol and Neurock[46] (*vide infra*) concluded that for adsorbates with large dipole moments and for kinetic stud-

ies the more sophisticated SC method should be applied.[45] However, to go beyond the CHE approach, one needs to explicitly integrate the electrochemical potential into the first principles calculations. Applying an electrochemical potential is equivalent to tune the workfunction, which is simulated by adding or subtracting electrons from the neutral system. Hence, charged systems are necessary to explicitly investigate the effect of an electrochemical potential on surface adsorbed species. Unfortunately, charged systems cannot be simulated under periodic boundary conditions, which most efficiently simulate extended metallic systems: a periodically charged system is infinitely charged and hence the Coulomb potential diverges. Therefore, when changing the number of electrons in periodic computations a countercharge is required. Several schemes have been proposed in the literature.[26,46–53] The technically simplest way to deal with the situation is to include a homogeneous background charge.[46] The technical simplicity leads to a major drawback: the uniform background charge interacts with the system, even within the metallic slab. Filhol and Neurock have proposed a correction, leading to the surface charging (SC) mehod, in order to mitigate the issue.[46,52] The SC model provides, despite the approximations, excellent agreement with experiment when a water bilayer is used to solvate the surfaces, as exemplified by the phase diagram of H_2O over Pt[45,54] and Ni[55], CO electro-oxidation over Pt[56] and the borohydride oxidation.[57]

In addition to the electrochemical potential, electrochemistry depends critically on the solvent because the dielectric constant of the solvent governs the capability of a system to stabilize and "store" charges, i.e., the capacitance of the system. Therefore, solvent effects are especially important for charged systems. So far, the water solvent was modeled using an explicit bilayer of water.[45,54–59] In our case, we aim at modelling an aprotic solvent such as DMF. However, just like including an electrochemical potential into the simulations, accounting for solvent effects in electronic structure computations of extended systems is still in its infancy,[60–63] with implicit solvent models becoming publically available only very recently.[64] This contrasts with the situation of molecular chemistry where several solvent models have been developed and applied for many years.[65]

The aim of this study is two-fold. On the one hand, we will provide some insight into the selectivity towards the formation of carbonates upon CO_2 electrolysis over nickel in aprotic conditions. On the other hand, we will elucidate the influence of the applied electrochemical potential on species adsorbed on a metal surface in order to clarify two aspects of the modelling of heterogeneous electrocatalysis: first, the importance to account explicitly for the electrochemical potential, going beyond the simplest consideration of the electrochemical potential and second the role of modelling the solvent.

The following section reminds the reader of the basics of

modelling electrochemistry, before discussing the advantages and limitations of the two schemes applied herein: the simple linear free energy relationship for the electron chemical potential (LFER-EP), popularized by Norskov and coworkers and the explicit change of the electrochemical potential through charging the surface and neutralizing the simulation cell with a homogeneous background charge (SC) as developped by Filhol and Neurock. After this methodological discussion, the results for aprotic CO_2 reduction as described by the two approaches are presented to illustrate the influence of the applied electrochemical potential and the solvation effects simultaneously. With the SC method, we investigate the origin of the selectivity of Ni(111) to produce carbon monoxide and carbonates rather than oxalates.

2 Methods

Computational modelling of electrochemistry is hampered by the simple fact that the electrode potential is not a natural variable in quantum chemical computations. Most chemists are used to think in the "constant charge" picture, i.e., the number of electrons is not fluctuating during a reaction. Since each species with a given number of electrons corresponds to a different electrochemical potential, the "constant charge" picture is inadequate for electrochemistry, where all the intermediates should be treated at the same potential. For example, CO_2 adsorbed on a metal surface corresponds to a different potential than CO and O co-adsorbed on the same surface. Hence, to get the correct reaction energy, the charge on the surface for adsorbed CO_2 and CO,O need to be adapted individually to reach the desired potential. Therefore, an electrochemical half-cell is effectively a grand-canonical ensemble where the number of electrons is adapted according to the electrochemical potential in a different way for different intermediates of an electrochemical reaction. The most realistic approach would be to account for solvent molecules and explicit counterions, but this approach is computationally very demanding, requiring large unit cells together with statistically meaningful sampling of the solvent and counterion positions. To overcome this challenge, more approximate schemes have been developed, where the countercharge is introduced as some idealized distribution in the unit cell (*vide infra*).

### 2.1 Basics of Electrochemistry

To set the stage, this section gives a brief reminder of the basic text book equations in electrochemistry, starting with the standard Gibbs energy of reaction $\Delta_r G^\ominus$

$$\Delta_r G^\ominus = -nFU^{SHE,\ominus} \tag{1}$$

where n is the number of electrons transferred, F the Faraday constant and $U^{SHE,\ominus}$ the standard reduction potential refer-

enced to the standard hydrogen electrode (SHE).

The SHE is an ideal electrode which is immersed in an aqueous solution with a H_2 and H^+ activity of unity and a zero overpotential for hydrogen evolution, which corresponds to the following definition

$$2H^+ + 2e^- \rightleftharpoons H_2 \quad \Delta_r G^\ominus = 0.0 \text{ at } U^{SHE} = 0 \text{ V} \tag{2}$$
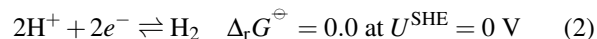
It is with respect to this idealized electrode reaction that formal "half-cell" potentials are commonly defined.

By definition, the reduction is occurring at the cathode and the oxidation at the anode, yielding the cell potential $U^\ominus_{cell}$

$$U^\ominus_{cell} = U^\ominus_{cathode} - U^\ominus_{anode} \tag{3}$$

Away from standard conditions, it is most straight forward to compute first $\Delta_r G$ of the reaction and then convert it back into a potential, also known as electromotive force, using the universal equation

$$U_{cell} = -\frac{\Delta_r G}{nF} \tag{4}$$

For spontaneous reactions, $\Delta_r G$ is negative and hence U_{cell} is positive.

When *applying* an electrochemical potential, it is helpful to work with the following equation

$$\Delta_r G(U^{SHE}) = -nF(U^{SHE,\ominus} - U^{SHE}) = \Delta G_r^\ominus + nFU^{SHE} \tag{5}$$

where U^{SHE} is the imposed potential and $U^{SHE,\ominus} - U^{SHE}$ is, in general, the over- or underpotential.

The SHE is inconvenient for computational purposes, as simulating the hydrogen evolution under realistic conditions and measuring potentials relative to this half-cell is extremely cumbersome. Therefore, the common computational reference state is vacuum: on the "vacuum scale", the energy of an electron in vacuum is defined as zero and all the attractive energy comes from interactions with the nuclei. This scale is often called the "absolute" scale for redox potentials; we will stick to the unambiguous term "vacuum scale".[66]

A concept closely related to the electrode potential on the vacuum scale is the workfunction W. The workfunction is the energy required to remove one electron from a surface, i.e., we can understand the workfunction as the ionization energy. For metals, the electron affinity and the ionization energy have the same value with opposite signs. Since the vacuum scale sets the energy of the electron in vacuum to zero, the chemical potential of the electron (μ_e) in the electrode is equal to minus the workfunction, whereas the workfunction is identical to the electrochemical potential, U^{vac}. Hence we might write

$$W = U^{vac} = -\mu_e \tag{6}$$

Of course, the "experimental scale", U^{SHE}, and the vacuum scale, U^{vac}, are related. IUPAC recommends[67] to assign a value of $U^{vac} = 4.44$ V to the standard hydrogen electrode.[70] Accordingly, we easily switch from one scale to the other using $U^{vac} = U^{SHE} + 4.44$ V as illustrated in Fig. 1. The remaining question is how a given computation is connected to one or the other scale.
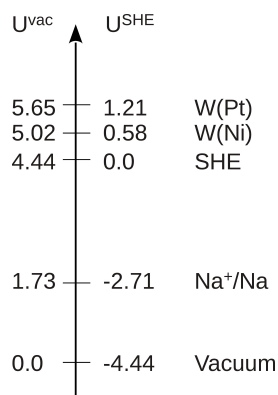

Fig. 1: Scales of the electrochemical potential in Volts with respect to the vacuum (left) and to the standard hydrogen electrode (right). The experimental Na/Na$^+$ redox couple and the computed workfunction of Ni(111) and Pt(111) are given as examples.

2.2 Linear Free Energy Relationship for Electrochemical Potentials

The linear free energy relationship for accounting for the electrochemical potential, LFER-EP, is the zeroth order level to treat electrochemical reactions, since it accounts exclusively for the energy of the transferred electron. The premise is that elementary reaction steps can be devided into chemical steps (where the composition of the system remains constant) and electrochemical steps, where the number of electrons changes due to adding/removing an electron and its cation (e.g., $Na^+ + e^- \rightleftharpoons Na_{(s)}$ or the more typical $H^+ + e^- \rightleftharpoons \frac{1}{2}H_2$). The LFER-EP has been introduced by Norskov and coworkers in the formulation of the computational hydrogen electrode (CHE).[35] Throughout this article, we will use LFER-EP for the generalization of the CHE to other cations than the proton.[36] However, in this section, the characteristics of the LFER-EP are discussed with the example of the CHE.

The model and assumptions of the CHE are summarized in the following:

1. Electronic energies are only required for electroneutral entities and thus do not depend on the electrochemical potential. When evaluating the potential dependence of

reaction energies, these "zero charge" results give the reaction energy at 0 V vs. SHE.[71]

2. Electron transfers are always coupled to proton transfers and no charged systems are involved. Therefore, processes that have no direct involvement of counterions (e.g., $Fe^{3+}(cp)_2 + e^- \rightarrow Fe^{2+}(cp)_2$ with cp=cyclopentadienyl) cannot be studied straightforwardly.

3. The applied electrochemical potential only affects the electrochemical steps, i.e., the proton coupled electron transfers.

4. The correction for the applied potential is derived from: $\Delta G_{H^+ + e^-}(U^{SHE}) = \frac{1}{2}\Delta G_{H_2}^{\ominus} - qU^{SHE}$. In other words, the energy of the electron in the electrode is equal to $-qU^{SHE}$, where q is the fundamental charge involved in the electrochemical step.

5. The choice of the reference electrode and how it is coupled to the system under consideration implies that the solvent is water and that the hydration energy of a proton is neither influenced by the electrochemical potential nor by the electrolyte.

To summarize, the computational hydrogen electrode allows to account for the nominal potential dependence of an electrochemical reaction, i.e., to account for the last term of Eq. 5, nFU. However, it disregards any influence of the interaction between species and the electrode itself at a specific potential, i.e., it describes the correct physics for solution phase electrochemistry, but it is an approximation for the elementary reaction steps on an electrified interface where the number of electrons is variable in order to impose the constant potential. Despite these limitations, the LFER-EP is not only extremely simple to apply (being an *a posteriori* correction to "standard" computations), but also the first step in any scheme improving on the LFER-EP.

2.3 Beyond the Linear Free Energy Relationship: The Surface Charging Method

Any method aiming to improve over the LFER-EP has to take the specific interactions between adsorbates and the electrified electrode explicitly into account, lifting assumptions 1-3 in the CHE (*vide supra*) by introducing $\Delta G_r^{elec}(U)$. The superscript "elec" indicates that the electronic contribution, originating in polarization and charge-transfer, to the free energy is included. The simplest approach to assess the importance of the applied electrochemical potential on the energies of adsorbates would be to apply an electrical field in the simulation cell.[72–74] However, the surface charge density q_{surf}, needed for obtaining the electrochemical free energy, is tricky to evaluate.[75]

Schemes that account for all relevant free energy changes alter, therefore, the number of electrons in the system explicitly[46,48,49,51–53,76] and work with the grand-canonical energy expression for all the surface adsorbed species. The potential dependent free energy of the surface $G_{\text{surf}}(U^{\text{vac}})$ is given by

$$\Delta G_{\text{surf}}(U^{\text{vac}}) = \Delta E_{\text{surf}}^{\text{elec}}(U^{\text{vac}}) - q_{\text{surf}}(U^{\text{vac}})FU^{\text{vac}}$$

$$\approx \Delta E_{\text{surf}}^{\text{elec}}(U_0) - \frac{1}{2}C(U^{\text{vac}} - U_0^{\text{vac}})^2 \qquad (7)$$

with $\Delta E_{\text{surf}}^{\text{elec}}(U^{\text{vac}})$ being the electronic energy at potential U^{vac} and q_{surf} is positive if electrons are removed and negative when electrons are added, i.e., q_{surf} is the surface charge density of the system and U^{vac} is the vacuum scale potential of the electrode. The reasoning behind Eq. 7 is that electrons removed from the system are transferred to the electrode which serves as the reservoir of electrons at the potential U^{vac}. Similarly, adding an electron from the electrode is associated with the energetic cost of removing the electron from the reservoir. The approximate equality refers to the quadratic development of the electronic free energy,[76,77] which can serve to introduce the notion of the capacitance C of the surface and simplifies the link between SC and LFER-EP results. Assuming a constant capacitance for a given surface (which is often a reasonable first order approximation[78]) the results of LFER-EP and Eq. 7 are identical at the potential which corresponds to the average of the zero charge potentials (U_0), i.e., the workfunctions. Note that in the SC model the capacitance C is not an "external" constant: its value, which corresponds to the curvature of the parabola (*vide infra*), is determined for each system independently and is thus quite different in vacuum than in implicit DMF. Furthermore, as can be seen in Fig. 6, the capacitance weakly depends on the adsorbate: the binding energy difference between two adsorbates (e.g., 2 CO_2 vs. CO,CO_3) are not simply straight lines as would be the case if the capacitances of the implicated systems were equal.

The different surface charging schemes (e.g., neutralization with a homogeneous background-charge as developed by Filhol and Neurock[46,52,76] or Otani's implicit counterelectrode[48,53]) have a different way to obtain the first term of Eq. 7, i.e., $\Delta E^{\text{elec}}(U^{\text{vac}})$, while the second term is, essentially, the same as the one needed for the nominal potential dependence, introduced in the previous section. Here, we will apply the surface charging method in the formulation by Filhol and Neurock which we abreviate by SC.[76]

The two main advantages of these general approaches are a) *Proper potential alignment:* since these methods work with the vacuum scale potential, assessed through workfunctions, the potential of *all* the systems are referenced to vacuum and properly aligned, i.e., changes in the workfunction due to adsorptions and reactions are fully taken into account. b) *Decoupling of electron and counterion transfer:* Eq. 7 does not make use of any counterion. Hence a potential dependence of

a system where only an electron transfer has occurred is easily accessible. For example, the potential dependence of CO_2 adsorption is readily evaluated with such a scheme, while it is a constant within the LFER-EP framework. To be explicit, the clear distinction between "chemical" and "electrochemical" steps makes place for a "gradual, nuanced" description, where the electrochemical potential fixes an electrode polarization, which requires a specific surface charge density, q_{surf}. Hence, the coupled electron cation transfer, which could be reasonably described by LFER-EP and be a good approximation in the case of covalent bond formation (e.g., C–H), becomes a special case, while in general the surface charge changes by a characteristic value for a given elementary reaction.

The energy of the reactants in the formally electrochemical steps are obtained like in the LFER-EP approach, i.e.,

$$\Delta G_{X+e^-}(U^{\text{vac}}) = \Delta G_X + q(U_X^{\text{vac},\ominus} - U^{\text{vac}}) \qquad (8)$$

where, $U_X^{\text{vac},\ominus}$ can be either obtained from experiment (e.g., 4.44 V for $\frac{1}{2}$ H_2) or from the computed workfunction (e.g., 2.74 V for $Na(100)$ in vacuum). The advantage of the later approach is that the workfunction of an uncharged sodium surface can be computed under the specific computational conditions, e.g., using the same solvent model, giving a "consistent" description. Of course, this standard redox-potential can also be applied in the LFER-EP.

3 Model

The electroreduction of CO_2 under aprotic conditions opens several reaction channels. Herein, we investigate the C–C coupling of CO_2, leading to oxalates

$$2\,CO_2 + 2Na^+ + 2e^-$$
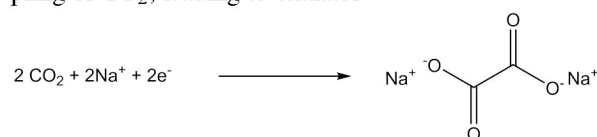
and the dissociation reaction of CO_2 into CO and adsorbed oxygen. Under electrochemical conditions, the surface bound oxygen may further be reduced to carbonate

$$2\,CO_2 + 2Na^+ + 2e^-$$
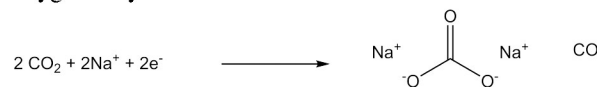
Both products are, in principle, competitors in any reaction where CO_2 is reduced electrochemically, e.g., formic acid or hydrocarbon formation[8,9,11,12,14,15] and are therefore worth studying in order to, subsequently, assess the selectivity of the target reactions. However, under the studied aprotic conditions, no formic acid or hydrocarbons can be formed.

As far as simulations are concerned, the aprotic solvent DMF has the advantage compared to water that is non-reactive and that no specific interactions (H-bonds) are expected between solvent and solute, but the disadvantage that its size is

considerably larger, pushing simulations with meaningful explicit layers of DMF beyond our present capabilities. However, the average effect of the solvent, i.e., increased capacitance, might be captured well enough by an implicit solvent model, which avoids the ambiguities in choosing a structure for the static solvent layers as usually proposed when including solvent effects.[46] Therefore, our study investigates the combination of implicit solvent treatment and explicit accounting of the electrochemical potential. Although this model is far from perfect (the double layer is grossly approximated by the homogeneous background charge and there are no explicit solvent molecules), to the best of our knowledge, it is the state of the art that can be done with publicly available, well established, periodic DFT codes.

We model the catalyst surface by the Ni(111) facet and the solvent by a continuum with a relative dielectric constant (ε) of 37.2, characteristic for DMF. The latter is also very close to the one of an other typical aprotic solvent for electrochemistry, acetonitrile ($\varepsilon = 37.7$). The results will hence be generally applicable to aprotic solvents with a high dielectric constant. Vlachos and co-workers concluded that the water gas shift reaction, which involves chemisorbed CO_2 and co-adsorbed CO,O similar to systems reported herein, yields overall similar results at the Ni(111) surface or the Ni(211) facet.[79] Therefore, we have limited ourselves to the ideal Ni(111) surface. In order to gain a more complete understanding, simulations over different surfaces and determination of activation barriers should be considered, but these investigations are beyond the scope of this study.

Experimentally, the electroreductive coupling of CO_2 to alkenes is carried out with a sacrifying aluminum or magnesium electrode.[16–18] Computationally, the monovalent sodium cation is more convenient than the di- or trivalent cations and the redox potential is comparable. Therefore, we model the counterion by Na^+. For example, carbonate is simulated as Na_2CO_3 instead of $Al_2(CO_3)_3$. The solvation energy of Na^+ is predicted to be -3.14 eV by the implicit solvation model. At the equilibrium potential, the energy of Na^+ in solution is equal to the energy of Na on the metallic sodium surface, i.e., the solvation energy is roughly compensated by the workfunction. The solvation energy provided by the implicit solvent model is, thus, fairly consistent with the workfunction of sodium metal (2.7 V) but shy of the 4-4.5 eV expected based on experimental data and cluster-continuum models in a similar solvent.[80] Considering that Na^+ is co-adsorbed on the surface (or embedded in the salt solid) and therefore never "fully solvated" and its energy is obtained from the workfunction of solid sodium, we did not try to improve the description of Na^+ by including explicit solvent molecules. Furthermore, the incurred error has an undetermined sign and magnitude compared to the experimentally relevant Al^{3+} or Mg^{2+}.

The salts (Na_2CO_3 and $Na_2C_2O_4$) are modelled as crystals with two chemical formulas per unit cell. These models are derived from experimental crystal structures[81,82] and are fully optimized.

To assess the window of the electrochemical stability of Na^+ under our conditions, there is, on the one hand, the workfunction of sodium (~ 2.7 V), which assures the formal stability of Na^+ down to about -1.8 V vs. SHE with respect to formation of solid sodium. On the other hand, Na^+ adsorption on Ni(111) is positive (i.e., unstable) within this potential window (*vide infra*, Fig. 2). Hence, Na^+ is, indeed, the relevant chemical species under the simulated conditions.

4 Computational Details

The metal surface is modeled as a symmetric p(3×3) Ni(111) slab with a lattice constant of 3.52 Å and a thickness of 5 layers (the middle layer is frozen in its bulk position), in a periodic box of 37.35 Å. The spin-polarized electronic structure is described at the PBE level,[83] with an energy cut-off of 400 eV for the plane-wave basis set. The electron–ion interactions are described by the PAW formalism.[84,85] All computations are performed with VASP 5.3.3.[86,87] Accounting for solvation effects is achieved by exploiting the implicit solvation model[26,88] as implemented by Hennig and co-workers under the name VASPsol.[64] In this model, the electrostatic interaction with the implicit solvent is computed based on a linear polarization model, where the relative permittivity of the medium is a continuous function of the electron density. A switching function around a specified isodensity value is used to vary the relative permitivity from 1 (well "inside" the surface metal atoms) to the solvent bulk value far away from the surface. This modified Hartree potential is obtained by solving the modified Poisson equation. Hence, the polarization of the system due to the solvent is included self-consistently. In order to get numerically stable results for the potential in empty space, the surface tension was set to zero (no cavitation energy) and the critical density value was reduced to 2.5 10^{-4} $e/Å^3$. The dielectric constant of DMF was set to 37.2. Note, that when we started this study, VASPsol was incompatible with non-local van der Waals density functionals and we did therefore not apply them. Since we are mainly comparing two electrochemical approaches, we do not expect to obtain qualitatively different conclusions upon accounting for weak non-bonded interactions. All geometries were optimized to reach a gradient smaller than 0.05 eV/Å with wave functions converged to $5\cdot10^{-5}$ eV. The precision setting of VASP is set to "normal" and the automatic optimization of the real-space projection operators is used.

The energy of the sodium cation is obtained according to Eq. 8 with the energy of an atom in bulk sodium (ΔG_{Na}) and the workfunction of the Na(100) surface ($U_{Na}^{vac,\ominus}$ is 2.74 V in

vacuum and 2.67 V in implicit DMF).

In the SC method, the system is charged and N_e electrons are present in total instead of the neutral N_0 number. In order to reach an overall neutral cell, a uniform background charge of opposite sign can be applied. This uniform charge is also present in the metal slab itself, where it is screened by the metal. Hence, the "effective" applied charge is reduced and the DFT energy must be corrected accordingly. The correction suggested by Filhol and Neurock[46,52,76] reads

$$G^{\text{elec}}(U^{\text{abs}}) = E_{\text{DFT}}(N_0) + \frac{z_0}{Z}\left(E_{\text{DFT}}(N_e) - E_{\text{DFT}}(N_0)\right)$$
$$+ \frac{z_0}{Z}\text{q}\int_{N_0}^{N_e} V_a(N_e)\text{d}N_e + U^{\text{abs}}(N_e - N_0) \quad (9)$$

where U^{abs} is the workfunction for the system with N_e electrons and N_0 is the number of electrons for the neutral system. Z is the interslab repeat vector of one supercell (z-direction) and z_0 is the segment along this direction not occupied by the metal slab (the radius of the atoms is derived from the lattice constant), therefore $\frac{z_0}{Z}$ (in our setup $\frac{z_0}{Z} = 0.703$) gives the ratio of the space in which the homogeneous back-ground charge is "active", i.e., not screened by the metallicity of the slab. This "screening" concerns $(N_e - N_0)\left(1 - \frac{z_0}{Z}\right)$ electrons. q is the elementary charge and the integral approximates the interaction energy of the homogeneous background with the system in order to remove this spurious interaction. The inter-action is estimated from the electrostatic potential V_a, in the middle between the two symmetric surfaces, which is taken to be the energy of the "vacuum", i.e., it is also used to com-pute the workfunction. Note, that even though we are using the symbol G for the free energy (to emphasize that the free energy change due to electron transfer is taken into account) Eq. 9 would need to be supplemented by the standard terms accounting for translational, rotational and vibrational degrees of freedom in order to be a "proper" Gibbs energy. When dis-cussing the results, we will thus refer to "adsorption energies" and not "adsorption free energies", although they are "elec-tronic free energies".

Energies were obtained for at least 5 different charges for each system. Subsequently, a parabolic fit was used for ac-cessing arbitrary potentials. The same procedure is applied to get the effective charge $q_{\text{surf}}(U)$ at an arbitrary potential. This data is used to evaluate the charge injection $\Delta^{\text{ads}}q(U) = \left(q_{\text{surf}}^{\text{slab}}(U) + N^{\text{mol}}\right) - q_{\text{surf}}^{\text{system}}(U)$ for a given reaction, where N^{mol} is the sum of the electrons in the isolated molecules (the counterion, Na^+, is considered as a charged species) adsorbed on the surface. A script for automating these tasks is avail-able in the supplementary information. Whenever technically possible, the charges were chosen to obtain an interpolating parabola between -2 and 1 V (vs SHE). Depending on the sys-tem this was not possible, as in the highly (negatively) charged systems the required electrons are not bound on the surface

anymore but spilling out into the "vacuum", filled with the background charge. In these situations, Eq. 9 is not applicable anymore, which is seen as strong deviations from the parabolic behavior.

5 Results and Discussion

CO_2 electrolysis under aprotic conditions is reported to yield CO and carbonate or the C–C coupling product, oxalate, de-pending on the electrode material. We therefore start by inves-tigating the adsorption of the reactant, CO_2, and its dissocia-tion into co-adsorbed CO and O. Then we consider the influ-ence of CO_2 coverage and the formation of oxalate, competing with the one of carbonate and carbon monoxide. Investigating this intrinsic reactivity of CO_2 under aprotic, reductive condi-tions will not only be helpful to understand the mechanism and selectivity of the carboxylation reaction of alkenes under sim-ilar conditions, but serves equally well to determine the level of modelling necessary to conduct such mechanistic studies for reactions where experimental results are scarce.

We compare the simple linear free energy relationship for the electrochemical potential (LFER-EP) to the more ad-vanced surface charging (SC) method. As explained above, LFER-EP does not describe the polarization of the surface and imposes a strict coupling of the Na^+ and e^- transfer. In contrast, the SC model polarizes the surface according the the electrochemical potential and electron transfer occurs also in the absence of a cation transfer. Hence, under strongly reduc-ing conditions SC and LFER-EP may differ significantly and SC is potentially more convenient: the cation (Na^+) has no well defined place in the reduced species (in contrast to the proton which forms regular C–H and O–H bonds), but has to be introduced in LFER-EP, while it might not be necessary in SC.

The adsorption of CO_2, together with the preferred adsorp-tion mode of oxalate on Ni(111) as a function of the potential will be used to assess the limitations of LFER-EP in prac-tice and the role of the solvent. Having established the con-sequences of the improved description of SC compared to LFER-EP, we investigate the coverage effect on CO_2 disso-ciative adsorption and elucidate the origin of the selectivity of CO and carbonate rather than oxalate formation over Ni(111).

5.1 Comparison of the Potential Dependence of Adsorp-tion Energies in Vacuum and Implicit Solvent

Fig. 2 shows the energetics and associated charge injection $\Delta^{\text{ads}}q$ in the case of CO_2 and Na^+ adsorption on Ni(111) as a function of the electrochemical potential in vacuum (left) and when accounting for solvent effects through an implicit sol-vent (right). The charge injection is defined as the net charge

(a) Adsorption energies
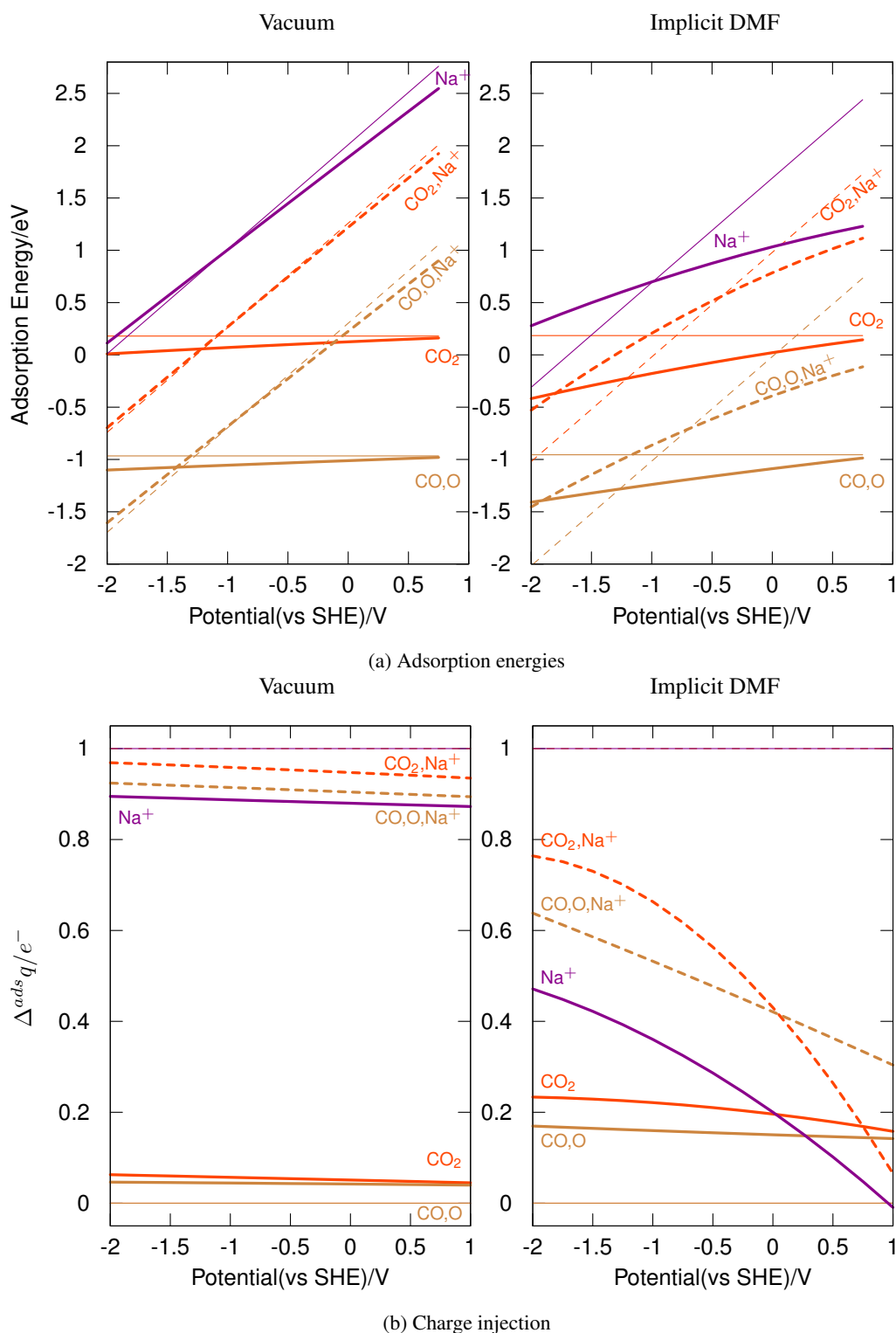
(b) Charge injection

Fig. 2: Adsorption (top) and associated charge injection (bottom) upon adsorption of Na^+ (purple) and of CO_2 on Ni(111) as a function of the electrochemical potential in vacuum (left) and implicit DMF (right). Two adsorption modes are compared for CO_2: the intact chemisorption (red) and the dissociative adsorption (i.e., CO and O co-adsorption, brown). Broken lines indicate the co-adsorption with Na^+. The thin lines refer to the LFER-EP, while the thick lines are computed with the SC method.

applied for the considered potential for the chemisorbed system minus that of the bare Ni(111) surface. It hence corresponds to the extra charge that needs to be injected in the presence of adsorbed species to maintain the potential constant. The LFER-EP framework is characterized by the distinction of elementary steps into "chemical" and "electrochemical" steps. The former are rearrangements of nuclear coordinates, while the latter involve addition/substraction of an electron and its counterion, e.g., $Na^+ + e^-$. Since electron and cation transfer are strictly coupled, the injected charge is simply 1 e^- for electrochemical steps and 0 for chemical steps. As a consequence, only the reaction energies of electrochemical steps depend on the potential within the LFER-EP approach. Furthermore, all systems are electroneutral. Within the SC model, however, the number of electrons in the system is individually adapted to every intermediate to tune the workfunction to the specified level. Therefore, the chemical and electrochemical steps are no longer formally separated from each other. In the text we will frequently refer to "oxalate" or "carbonate" for species adsorbed on the surface. These adsorbates do not necessarily have the "net" charge of the corresponding solution species: adsorbate and electrode form one system and the (surface) charge is a continuous function of the electrochemical potential.

We start the comparison of the two methods for including the electrochemical potential first in vacuum and only in a second stage when accounting for solvent effects.

As a first example for a chemical step, consider the adsorption of CO_2 in the absence of Na^+ co-adsorption: by construction, LFER-EP yields an adsorption energy which is independent on the potential and the injected charge is strictly 0. However, when co-adsorbing CO_2 with Na^+, we are confronted with an electrochemical step within the LFER-EP framework, since cation and electron transfer are coupled. The adsorption energy as a function of the potential has a slope of one, corresponding to the coupled electron transfer. In the case of the SC model, the surface charge adapts to the potential. However, since charges are not well stabilized in vacuum, the charge variations compared to LFER-EP (strict coupling of electron and cation transfer), obtained with the surface charging method, are almost negligible (Fig. 2b): the maximum difference occurs for Na^+ where the charge injection is ~ 0.9 instead of 1. The number of injected electrons is the main factor determining the potential dependence: according to Eq. 5 the slope of $\Delta G(U)$ is, to first order, proportional to the number of electrons injected. The inability of vacuum to stabilize charges implies that minor charge variations change the potential considerably, leading to very small free energy changes due to potential alignment effects. Since at the same time the electrons are only marginally better stabilized in one system than in the other (e.g., on $CO_2@Ni(111)$ compared to the bare surface), the adsorption energies barely change compared to

the zero charge (LFER-EP) results. In vacuum, the systems are thus effectively electroneutral and introducing a counterion is strongly coupled to an electron transfer. Hence, the potential dependence for the more detailed SC method is very similar to the simple LFER-EP method, i.e., adsorption in the absence of Na^+ are basically horizontal lines, while the reductive Na^+ adsorption or co-adsorption leads to a strong potential dependence with a slope ~ 1. Therefore, in vacuum, where charge accumulation at metals is small, the LFER-EP is a very reliable approximation.

Accounting for solvent effects leads to a very different picture when explicitly tuning the electrode potential, while the LFER-EP lines are quite similar to the ones in vacuum: on Fig. 2a (right) slopes of the thin lines are unchanged by construction, while intercepts are only affected in the case of Na^+ adsorption where the charge distribution is somewhat stabilized by the polarizable solvent. When applying the surface charging method, the dielectric medium stabilizes charges at the interface, especially in the presence of adsorbates and as a result the injected charge significantly deviates from the ideal values of zero or 1. Equivalently one might say that the dielectric medium increases the capacitance of the system. For chemisorbed CO_2 or CO,O, the injected charge is significantly enhanced by the solvent, up to a value of $\sim 0.2e^-$, and hence the adsorption energy depends on the potential with a marked stabilization at negative potentials, where CO_2 or CO accumulate a negative charge, which is stabilized by the solvent (Bader charges on the adsorbate as a function of the potential and the solvent can be found in the SI). Such a potential dependence is obviously absent in the LFER-EP, Hence, the two methods considerably deviate in the presence of a solvent. For example, at $U = -1$ V CO_2 is underbound by 0.4 eV compared to the SC method, which gives an exothermic reaction for CO_2 adsorption below 0 V.

Assuming a constant capacitance (C, see Eq. 7), lines for SC and LFER-EP cross at the average zero charge potential, i.e., at the potential that corresponds to the average of the workfunction of the neutral systems. Note that such an assumption is not involved in the SC model, but might be made for interpretative purposes. For example, the workfunction of Ni(111) and $CO_2@Ni(111)$ is 0.58 and 1.39 V vs. SHE in implicit DMF, respectively (see SI). Hence, the thin and thick full orange-red lines in the graph on the right of Fig. 2a are expected to cross at 0.99 V. Indeed, at 0.75 V (the limit of the x-axis in Fig. 2a), the two lines almost cross. The good agreement between the constant C prediction and the actual crossing point gives credibility to the approximation of constant capacity when comparing similar systems. Furthermore, this observation justifies to call the potential at the crossing point the effective potential to which the LFER-EP results of non-electrochemical steps corresponds to. Hence, the LFER-EP result for CO_2 adsorption in the absence of Na^+ co-adsorption

corresponds to an effective potential of almost 1 V, which is very far from the reducing conditions of interest herein.

The potential dependence of the Na^+ assisted adsorptions is also considerably modified by the solvent. The injected charge is markedly lower than 1 for Na^+ adsorption since the polar solvent stabilizes the partial positive charge on Na. This can be easily explained considering a particular case. Neutral $Na@Ni(111)$ corresponds to a potential of -2.6 V. At this potential, the bare surface is, however, not neutral, but effectively charged by 0.5 e^- for a p(3x3) super cell. Hence, the injected charge to reach the neutral $Na@Ni(111)$ is only 0.5 e^-. The co-adsorption of Na^+ and CO_2 combines the effects described above and the charge injection (although not complete to -1) reaches $\sim 0.75e^-$ at strongly reducing potentials. In other words, Na^+ adsorption is not coupled anymore with a full electron transfer and we are dealing with a somehow solvated Na^+ and partially reduced carbon dioxide. Similarly, in the case of CO_2 dissociation, there is only a rather weak potential dependence. Nevertheless, in both competing reactions, we clearly obtain a stronger potential dependence in the presence of the counterion than in its absence, demonstrating the stabilizing capabilities of counterions without imposing counterion-coupled electron transfers, provided that ionic species are stabilized in a dielectric medium. The partial injected charge in realistic solvent conditions and their deviation from the ideal values of 0 or 1 has strong consequences on the slope of the adsorption energy as a function of potential energy, that markedly differ between the two methods as seen on Fig. 2a right. Obviously, in the presence of a high dielectric constant solvent, the LFER-EP is not anymore a reliable approximation to evaluate adsorption energies.

5.2 Preferred Surface Species and Coverage Dependence of CO_2 Adsorption

In the following section, we will focus more closely on the nature of the preferred surface species as a function of the electrochemical potential. Independent on the scheme and conditions, the dissociative adsorption of CO_2 into CO and O is favored by at least 1 eV at low coverage (1/9 ML), motivating us to investigate higher coverages. Increasing the coverage also allows to model carbonate and oxalate formation since they require at least two CO_2 molecules in the unit cell, which corresponds, in our case to a coverage of 2/9 ML.

As seen in the previous section, SC delivers a more general description of the electrochemical systems than LFER-EP, provided solvation is included. Here, we are discussing the extreme case of dissociative adsorption of CO_2 in the absence of Na^+ co-adsorption as a function of the surface coverage. By construction, LFER-EP gives constant adsorption energies for these reactions. Furthermore, CO,O co-adsorption at zero charge has a workfunction of 1.37 V vs. SHE. Hence, the

LFER-EP result for the dissociative adsorption corresponds to an effective potential of about 1 V, just like $CO_2@Ni(111)$ (*vide supra*). This oxidative potential is far from the potentials of interest herein and we will thus not consider LFER-EP any further in this section. In the SC model, we can compute the Bader charges as a function of the potential (see SI). This analysis reveals that the charge on the surface bound oxygen varies less than the charge on CO when lowering the potential: the oxygen is already negatively charged like in a surface oxide and does not accept significantly more electrons. CO_3 is, on the other hand, a rather powerful electron acceptor and hence the injected charge is significantly higher when a CO_2 is coupled to a surface oxygen atom instead of being dissociated into CO,O (blue compared to brown lines in Fig. 3b). With the solvent taken into account, the charge injection reaches up to 0.5 electrons for carbonate at the highest coverage considered. This significant charge injection goes along with a dramatic stabilization of the species at reducing potentials, not only compared to the LFER-EP results, but also compared to other surface bound species. For example carbonate and CO at high coverages (full, blue line in Fig. 3b) gets more stable than dissociated CO_2 at 2/9 ML (broken, brown line) at potentials < -1.2 V.

This comparison shows that solvent effects are crucial for the prediction of relative stabilities under electrochemical conditions and to allow rather decoupled electron transfers. Hence, for chemical conclusions only SC results with a solvent description are discussed.

Increasing the CO_2 coverage from 1/9 to 3/9 ML (see Fig. 3a) goes along with a reduced tendency (per CO_2 molecule) to dissociate CO_2. Dissociative CO_2 adsorption is even endothermic at a coverage of 3/9 ML for potential > -0.5 V, while at 2/9 ML the CO_2 dissociation is exothermic, but already less than twice the value for 1/9 ML. Comparing the dissociated systems with the ones where carbonate is formed ($CO_2 + O \rightarrow CO_3$), a contrasting picture emerges. At a coverage of 2/9 ML carbonate formation (without counterions) is still disfavored at all potentials considered, but if a coverage of 3/9 ML is imposed, carbonate formation is expected even at mildly positive potentials. Furthermore, since the full, blue line crosses the broken brown line in Fig. 3a right, the thermodynamically preferred state switches with the potential: from dissociated CO_2 at an intermediate coverage (2/9 ML) for potentials > -1.2 V to carbonate and dissociated CO_2, yielding higher coverages (3/9 ML), for potentials < -1.2 V. The latter is in fair agreement with the report of carbonate formation starting around -1.5 V.[15,19,89] Nevertheless, even at 3/9 ML coverage, the dissociative adsorption of CO_2 is exothermic at potentials below -0.5 V in solution, suggesting that CO might generally be a relevant intermediate in CO_2 reduction over Ni, e.g., even for C–C bond formation with alkenes.

From a chemical point of view we have learned two lessons:

(a) Adsorption energies

(b) Charge injection

Fig. 3: Total adsorption energies (top) and associated charge injection (bottom) of one, two and three CO_2 on Ni(111) as a function of the electrochemical potential. The adsorbed species are derived from dissociated CO_2, i.e., CO and O (in brown), and at higher coverages, CO and CO_3. Three coverages are considered: 1/9 ML (spaced broken lines), 2/9 ML (broken lines) and 3/9 ML (full lines) in vacuum (left) and implicit DMF (right). The lines in blue correspond to systems where one CO_2 has reacted with a surface adsorbed oxygen atom to give CO_3. Thin lines refer to LFER-EP and thick lines to the SC method.

first, CO_2 has a strong thermodynamic tendency to dissociate on Ni(111) at any potential considered. Nevertheless, strongly reducing conditions are required to desorb reduced products (*vide infra*), i.e., the dissociation at anodic potentials is not catalytic but just poisoning the catalyst surface. This tendency to dissociate CO_2 is well in line with the frequently reported CO production during CO_2 electroreduction over Ni[15,19,89] and the use of Ni as a catalyst at the cathode of solid oxide electrolyzers of CO_2.[90] Second, thermodynamically, the surface bound oxygen can be coupled to a second CO_2 molecule yielding carbonates - and carbonate formation is favored at reducing potentials and high surface coverage.

5.2.1 Adsorption Mode of Oxalate Above, we have focused on CO_2 dissociation and the formation of a C–O bond. As an alternative, the reductive dimerization, i.e., the C–C bond formation yielding oxalate, has to be considered. When comparing the relative stability of C_2O_4 with CO_3,CO on Ni(111) one finds that oxalates are much higher in energy than carbonates, which is largely due to the important CO adsorption energy. Nevertheless, the adsorption mode of oxalates serves as an example for a switch in the preferred adsorption mode (as opposed to a switch in the preferred surface species) as a function of the electrochemical potential. Such a switch is, by definition, absent in the LFER-EP and thus illustrates the truly atomic, detailed understanding which is obtained with the SC method.
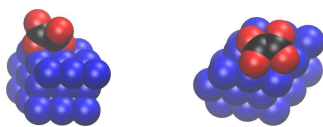

Fig. 4: "Perpendicular" and "parallel" adsorption mode of oxalate (C_2O_4) on Ni(111) on the left and right, respectively.

Fig. 4 shows the geometries of oxalates either adsorbed "flat", parallel, to the Ni(111) surface or slightly twisted, "perpendicular", creating a strong surface dipole and Fig. 5 shows their adsorption energies. The different magnitude of the surface dipole is also reflected by the workfunction, which is 1.52 and 1.78 V vs SHE for the parallel and perpendicular adsorption mode, respectively. The first observation is that with or without implicit solvent, the parallel adsorption mode is favored in the zero charge picture, which is what would be discussed in the context of the LFER-EP. However, when accounting for the potential dependence of the two adsorption modes, a crossing is obtained: in vacuum, quite reducing potentials (< -1.1 V) are necessary to stabilize the perpendicular mode. However, when accounting for the solvent, the situation is completely reversed: for potentials as high as 0.5 V the "perpendicular" mode is more stable, as now the charge accumulation "far" from the surface is stabilized by the solvent.

In addition, the energy of the adsorbed species is markedly modified. For example, the surface charging method stabilizes oxalate by 0.7 eV at -1 V compared to the zero charge picture.

Unfortunately, this implies that the "zero charge" relative stabilities (here a difference of about 0.2 eV) are not necessarily representative for the relative stabilities under electrochemical conditions. Therefore, even for the "conformational search" the potential dependence would need to be accounted for. However, since this is associated with substantial effort, we have limited ourselves herein to the lowest adsorption energy at zero charge. Further studies will try to establish a rapid pre-screening or "predictive" scheme which exploits the workfunction differences between competing adsorption modes in order to identify the structures for which computing the potential dependence is warranted.

5.3 Reaction Energies for Carbonate and Oxalate Formation

Carbonates are possibly formed at high coverages, even in the absence of counterions. On the other hand, the simplest C–C coupling product, oxalate, seems to lie at considerably higher energy. These findings raise the question: with the possibility of stabilizing counterions, would carbonate form quantitatively or could oxalate be dramatically stabilized?

To start with, we consider the reaction energy of the overall reactions starting from CO_2 in gas-phase

$$2CO_2(g) + 2(Na^+ + e^-) \rightarrow Na_2CO_3(s) + CO(g)$$

$$2CO_2(g) + 2(Na^+ + e^-) \rightarrow Na_2C_2O_4(s)$$
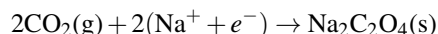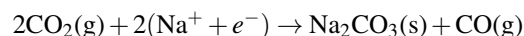
yielding the $Na_2CO_3(s)$ and $Na_2C_2O_4(s)$ salts, which are, for computational efficiency, modelled by perfect periodic crystals (see section Models). These salts are dissolved by high dielectric solvents such as DMF. Hence, their true energy (e.g., as ion pairs in solution) is lower than assumed herein. These reaction energies are given as a function of the potential in thin broken lines in Fig. 6. For sake of consistency with the adsorption energies discussed above, reaction energies are "electronic" energies, i.e., neglecting zero-point and thermal corrections.

If the overall reaction is uphill at potential U, then the reaction is unlikely to proceed at room temperature. Hence, we first investigate the overall thermodynamics of quantitative formation of crystalline sodium carbonate and sodium oxalate starting from CO_2, Na^+ and electrons at a potential U that is sufficiently reductive (see broken lines in Fig. 6). In the case of carbonates, the side product is carbon monoxide, which has to be desorbed from the surface in order to close the catalytic cycle. This step is endothermic by about 1.9 eV and therefore the formation of crystalline sodium carbonate requires
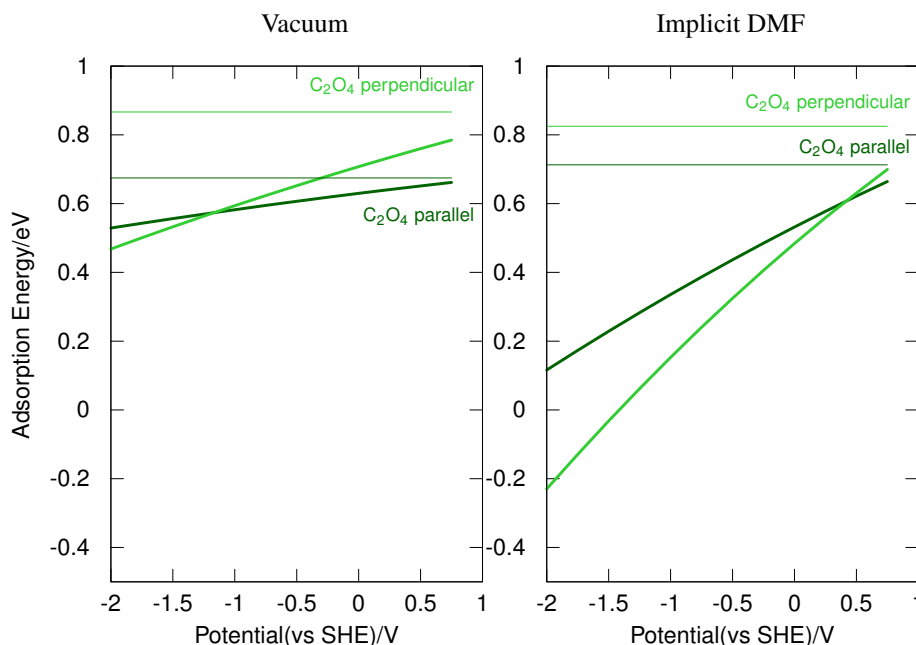
Fig. 5: Adsorption energies of two CO_2 molecules, in the form of oxalate as a function of the electrochemical potential. The oxalate can be adsorbed "parallel" to the nickel surface (dark green) or perpendicular (green). Thin lines refer to the zero charge picture while broken lines refer to the surface charging method. The graph on the left and right correspond to vacuum and implicit DMF, respectively.

a minimal potential of -1.25 V for the combined reaction to be exothermic, in reasonable agreement with the reported onset potential around -1.5 V.[15] Oxalate formation, on the other hand, is thermodynamically much more accessible: already at potentials lower than -0.6 V, the formation of sodium oxalate is thermodynamically feasible.

Since both carbonate and oxalate formation are surface assisted processes, the second relevant question is if these reactions are feasible on the surface. Hence, we investigate the transformation of chemisorbed CO_2 to adsorbed products. Depending on the potential, the reactant and/or the products are co-adsorbed with Na^+ and the corresponding SC reaction energies are represented in thick lines in Fig. 6. Concerning the reactant, the co-adsorption of CO_2 with Na^+ is favored at stronlgy reducing potentials. This change in the energy reference leads to a discontinuity in the reaction energies and is indicated by a vertical line Similarly, for each segment, the most stable product is indicated on Fig. 6 at the given coverage (i.e. 2/9 ML): the number of co-adsorbed Na^+ increases with more and more reducing (more negative) potentials. These changes of the number of cations lead to the other discontinuities in the reaction energy. Since we are considering reaction energies, the reference energy is different from that of the preceding figures, which modifies the aspect of the potential dependence. The potential dependence of relative energies is

directly related to the difference in workfunction. The change in workfunction (potential of zero charge) is often larger for an adsorption process than for a surface reaction. Therefore, the potential dependence of reaction energies is often less pronounced than for adsorption energies. Nevertheless, since the workfunction still changes during a reaction, the SC method delivers more reliable results in general and we are only showing and discussing these results.

The oxalate formation is shown as a green line in Fig. 6: at potentials > -0.5 V, Na^+ does neither co-adsorb with the reactant nor with the product in vacuum and formation of oxalate on the surface is endothermic. For lower potentials, one counterion is co-adsorbed with oxalate, but not with CO_2, giving rise to the noticeable potential dependence of the reaction energy. Furthermore, at potentials lower than -0.9 V, the surface catalyzed reaction could take place at a reasonable rate since it is exothermic, provided that there is chemisorbed CO_2 available and not only CO and O. At potentials lower than -1.25 V, the reactant is CO_2, co-adsorbed with Na^+ that yields surface adsorbed sodium oxalate ($Na_2C_2O_4$). However, the potential dependence of the elementary reaction is almost negligible in the absence of Na^+ co-adsorption, i.e., the capacitance and workfunction of C_2O_4@Ni(111) is not significantly larger than that of CO_2@Ni(111). The situation for carbonate formation is similar as for oxalate formation, except that ther-
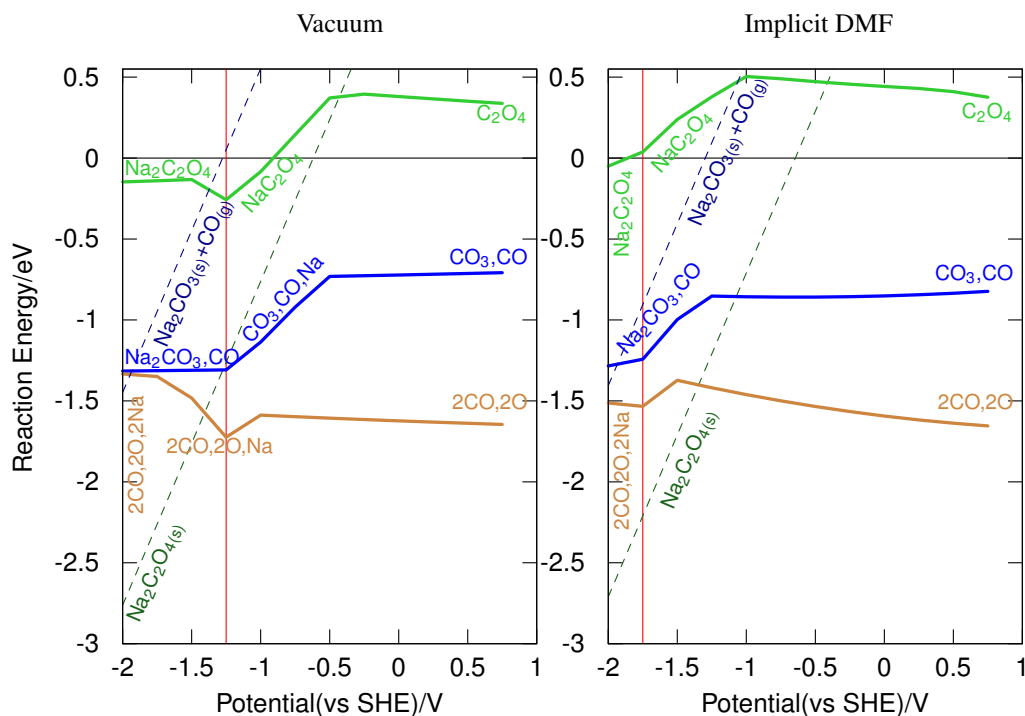
Fig. 6: Reaction energies of two CO_2 as a function of the electrochemical potential in vacuum (left) and implicit DMF (right). Thick lines refer to reactions starting from chemisorbed CO_2 yielding adsorbed products, e.g., CO_3,CO (blue): $2\,CO_2^{ads} \rightarrow CO,CO_3^{ads}$, with the number of co-adsorbed Na^+ adapted according to the potential. Thin lines refer to the overall reaction: isolated CO_2 reacts with electrons and counterions to yield precipitated salts, e.g., $Na_2C_2O_{4(s)}$ (dark-green): $2\,CO_2(g) + 2\,Na^+ + 2\,e^- \rightarrow Na_2C_2O_{4(s)}$. The vertical red lines indicate the point where the reactant changes from CO_2,Na@Ni(111) to CO_2@Ni(111).

modynamically it is much more accessible on the surface, not the least because of the CO@Ni(111) byproduct. Hence, carbonate formation is preferred over oxalate formation on the Ni(111) surface, although the overall reaction energy is less favorable. Nevertheless, the dominating surface species down to -1.75 V is CO,O, which itself might react with additional CO_2 to yield carbonate, but is not expected to form oxalates.

Na^+ co-adsorption provides less stability under solvent conditions than in vacuum. For instance, surface adsorbed oxalate is stabilized by Na^+ at potentials below -0.5 V in vacuum, but only below -1.0 V in implicit DMF. As a consequence, the surface reaction forming C_2O_4 is isoenergetic at ∼-0.9 V in vacuum, but it takes -1.9 V when solvating the systems. Hence, oxalate formation on Ni(111) is even less expected under solvent conditions than in vacuum. Furthermore, adsorbed oxalate is more compact and thus less accessible to the solvent than two chemisorbed CO_2 molecules, resulting in a loss of solvation energy for oxalate formation. Although similar remarks apply to carbonate formation, the details differ slightly, mostly because the solvent effect is enhanced for carbonate compared to oxalate. Finally, the relative stability

of CO,O (2/9 ML) compared to carbonate in solvent varies less with the potential than in vacuum. Nevertheless, at very reducing potentials carbonate formation becomes competitive with the poisoning of the catalyst by the CO,O surface layer, just like in vacuum. Hence, the combination of unfavorable oxalate formation on the surface with the overwhelming competition of CO_2 dissociation and carbonate formation makes oxalate formation unlikely over a nickel catalyst despite a favorable overall reaction energy. In contrast, carbonate and carbon monoxide formation is likely at low potentials. This selectivity between the two possible products of CO_2 electroreduction under aprotic conditions over Ni is in excellent agreement with experimental observations: oxalate formation accounts for less than 10% of the current density, while CO formation is the major product observed under aprotic conditions.[11,14,15]

6 Conclusion

Investigating by first principles the intrinsic reactivity of CO_2 on Ni(111) under electrochemically reducing conditions in

aprotic media, we have compared two approaches that take the electrochemical potential into account. Furthermore, the comparison exploits a recently implemented implicit solvent model[64] to move towards more realistic conditions than vacuum.

The present study evidences that the zeroth order method for including the electrochemical potential (LFER-EP) is a valuable tool to quickly assess the thermodynamic aspects of electrocatalysis in vacuum, which often gives a good indication of the processes under more realistic conditions. For example, this highly efficient approach correctly identifies the dissociative adsorption of CO_2 yielding CO and O as exothermic at all relevant potentials and predicts the formation of carbonates, rather than oxalates, over Ni(111). This preference is due to an insufficiently stabilizing interaction of oxalate with the surface. The surface charging method (SC) allows to vary the charge on the adsorbates as a function of the potential. Therefore, in contrast to the LFER-EP, which is limitted to cation coupled electron transfers, the SC method stabilizes the chemisorption of CO_2 at reducing potentials even in the absence of counterions. While the LFER-EP results are insensitive to the inclusion of an implicit solvent description, the situation is dramatically modified when explicitly accounting for the electrochemical potential by charging the electrode. The solvent strongly increases the capacitance of the surface and hence the surface charge for a given bias potential. Even the rather simplistic solvation model applied herein gives rise to marked changes in electrochemical reactivity compared to vacuum. Most strikingly, the charge injection is system dependent and differs significantly from the ideal values of 0 and 1. As a consequence, adsorption energies are potential dependent when accounting for solvent effects. This results, even in the absence of counterion co-adsorption, in a potential dependence of the most stable surface species, e.g., formation of carbonates rather than just CO and O for coverages above 2/9 ML, and the preferred adsorption mode of oxalate, while such a dependency is inherently absent in LFER-EP. In summary, the SC method coupled with an implicit solvent model gives access to a wealth of detailed information beyond the LFER-EP. Therefore, we recommend this more advanced, but still quite efficient, model when seeking an understanding of the fundamental processes in an electrochemical interfacial system.

References

1 K. S. Joya, Y. F. Joya, K. Ocakoglu and R. van de Krol, *Angew. Chem. Int. Ed.*, 2013, **52**, 10426.

2 A. J. Appleby, *Catalysis Reviews*, 1971, **4**, 221.

3 J. Bockris, *Int. J. Hydrogen Energy*, 1999, **24**, 1.

4 N. S. Lewis and D. G. Nocera, *Proc. Natl. Acad. Sci.*, 2006, **103**, 15729.

5 J. O. Bockris, *Int. J. Hydrogen Energy*, 2008, **33**, 2129.

6 D. Pletcher and J. Girault, *J. Appl. Electrochem.*, 1986, **16**, 791.

7 J. Bringmann and E. Dinjus, *Appl. Organometal. Chem.*, 2001, **15**, 135.

8 M. Gattrell, N. Gupta and A. Co, *J. Electroanal. Chem.*, 2006, **594**, 1.

9 Y. Hori, *Modern Aspects of Electrochemistry*, Springer, New York, Gaithersburg MD, 20899, 2008, ch. 3, p. 89.

10 D. Canfield and K. W. Frese, *J. Electrochem. Soc.*, 1983, **130**, 1772.

11 S. Ikeda, T. Takagi and K. Ito, *Bull. Chem. Soc. Jpn.*, 1987, **60**, 2517.

12 D. T. Whipple and P. J. A. Kenis, *J. Phys. Chem. Lett.*, 2010, **1**, 3451.

13 I. Ganesh, *Renewable and Sustainable Energy Reviews*, 2014, **31**, 221.

14 M. Jitaru, D. Lowy, M. Toma, B. Toma and L. Oniciu, 1997, **27**, 875.

15 J.-P. Jones, G. K. S. Prakash and G. A. Olah, *Isr. J. Chem.*, 2014, **54**, 1451.

16 G.-Q. Yuan, H.-F. Jiang, C. Lin and S.-J. Liao, *Electrochim. Acta*, 2008, **53**, 2170.

17 C.-H. Li, G.-Q. Yuan, X.-C. Ji, X.-J. Wang, J.-S. Ye and H.-F. Jiang, *Electrochim. Acta*, 2011, **56**, 1529.

18 R. Matthessen, J. Fransaer, K. Binnemans and D. E. D. Vos, *RSC Adv.*, 2013, **3**, 4634.

19 T. Yamamoto, D. A. Tryk, K. Hashimoto, A. Fujishima and M. Okawa, *J. Electrochem. Soc.*, 2000, **147**, 3393.

20 O. M. Magnussen, J. Hotlos, R. J. Nichols, D. M. Kolb and R. J. Behm, *Phys. Rev. Lett.*, 1990, **64**, 2929.

21 T. Iwasita and F. Nart, *Prog. Surf. Sci.*, 1997, **55**, 271.

22 K. Jambunathan and A. C. Hillier, *J. Electrochem. Soc.*, 2003, **150**, E312.

23 K. Jambunathan, S. Jayaraman and A. C. Hillier, *Langmuir*, 2004, **20**, 1856.

24 Y. X. Chen, M. Heinen, Z. Jusys and R. J. Behm, *Angew. Chem., Int. Ed.*, 2006, **45**, 981.

25 Y. Gorlin, B. Lassalle-Kaiser, J. D. Benck, S. Gul, S. M. Webb, V. K. Yachandra, J. Yano and T. F. Jaramillo, *J. Am. Chem. Soc.*, 2013, **135**, 8525.

26 K. Letchworth-Weaver and T. A. Arias, *Phys. Rev. B*, 2012, **86**, 075140.

27 J. I. Siepmann and M. Sprik, *J. Chem. Phys.*, 1995, **102**, 511.

28 S. Tazi, M. Salanne, C. Simon, P. Turq, M. Pounds and P. A. Madden, *J. Phys. Chem. B*, 2010, **114**, 8453.

29 D. M. Bernardi and M. W. Verbrugge, *J. Electrochem. Soc.*, 1992, **139**, 2477.

30 W. Goddard, B. Merinov, A. van Duin, T. Jacob, M. Blanco, V. Molinero, S. Jang and Y. Jang, *Mol. Simul.*, 2006, **32**, 251.

31 R. Ferreira de Morais, P. Sautet, D. Loffreda and A. A. Franco, *Electrochim. Acta*, 2011, **56**, 10842.

32 K. Ito, S. Ikeda, N. Yamauchi, T. Iida and T. Takagi, *Bull. Chem. Soc. Jpn.*, 1985, **58**, 3027.

33 L. Sun, G. K. Ramesha, P. V. Kamat and J. F. Brennecke, *Langmuir*, 2014, **30**, 6302.

34 B. Eneau-Innocent, D. Pasquier, F. Ropital, J.-M. Leger and K. B. Kokoh, *Applied Catalysis B: Environmental*, 2010, **98**, 65.

35 J. K. Norskov, J. Rossmeisl, A. Logadottir, L. Lindqvist, J. R. Kitchin, T. Bligaard and H. Jonsson, *J. Phys. Chem. B*, 2004, **108**, 17886.

36 J. S. Hummelshoj, J. Blomqvist, S. Datta, T. Vegge, J. Rossmeisl, K. S. Thygesen, A. C. Luntz, K. W. Jacobsen and J. K. Norskov, *J. Chem. Phys.*, 2010, **132**, 071101.

37 J. Greeley, J. K. Norskov and M. Mavrikakis, *Annu. Rev. Phys. Chem.*, 2002, **53**, 319.

38 V. Stamenkovic, B. S. Mun, K. J. J. Mayrhofer, P. N. Ross, N. M. Markovic, J. Rossmeisl, J. Greeley and J. K. Norskov, *Angew. Chem., Int. Ed.*, 2006, **45**, 2897.

39 J. Rossmeisl, Z.-W. Qu, H. Zhu, G.-J. Kroes and J. Norskov, *J. Electroanal. Chem.*, 2007, **607**, 83.

40 P. Ferrin, A. U. Nilekar, J. Greeley, M. Mavrikakis and J. Rossmeisl, *Surf. Sci.*, 2008, **602**, 3424.

41 J. Greeley, S. I. E. L., A. S. Bondarenko, T. P. Johansson, H. A. Hansen, T. F. Jaramillo, J. Rossmeisl, I. Chorkendorff and J. K. Norskov, *Nat. Chem.*, 2009, **1**, 552.

42 J. A. Keith, G. Jerkiewicz and T. Jacob, *ChemPhysChem*, 2010, **11**, 2779.

43 I. C. Man, H.-Y. Su, F. Calle-Vallejo, H. A. Hansen, J. I. Martinez, N. G. Inoglu, J. Kitchin, T. F. Jaramillo, J. K. Norskov and J. Rossmeisl, *Chem-CatChem*, 2011, **3**, 1159.

44 A. S. Bandarenka, A. S. Varela, M. Karamad, F. Calle-Vallejo, L. Bech, F. J. Perez-Alonso, J. Rossmeisl, I. E. L. Stephens and I. Chorkendorff, *Angew. Chem. Int. Ed.*, 2012, **51**, 11845.

45 J. Rossmeisl, J. K. Norskov, C. D. Taylor, M. J. Janik and M. Neurock, *J. Phys. Chem. B*, 2006, **110**, 21833.

46 C. D. Taylor, S. A. Wasileski, J.-S. Filhol and M. Neurock, *Phys. Rev. B*, 2006, **73**, 165402.

47 A. Y. Lozovoi and A. Alavi, *Phys. Rev. B*, 2003, **68**, 245416.

48 M. Otani and O. Sugino, *Phys. Rev. B*, 2006, **73**, 115407.

49 R. Jinnouchi and A. B. Anderson, *Phys. Rev. B*, 2008, **77**, 245417.

50 I. Dabo, B. Kozinsky, N. E. Singh-Miller and N. Marzari, *Phys. Rev. B*, 2008, **77**, 115139.

51 Y.-H. Fang and Z.-P. Liu, *J. Phys. Chem. C*, 2009, **113**, 9765.

52 M. Mamatkulov and J.-S. Filhol, *Phys. Chem. Chem. Phys.*, 2011, **13**, 7675.

53 I. Hamada, O. Sugino, N. Bonnet and M. Otani, *Phys. Rev. B*, 2013, **88**, 155427.

54 J.-S. Filhol and M. Neurock, *Angew. Chem., Int. Ed.*, 2006, **45**, 402.

55 C. Taylor, R. G. Kelly and M. Neurock, *J. Electrochem. Soc.*, 2006, **153**, E207.

56 M. J. Janik and M. Neurock, *Electrochim. Acta*, 2007, **52**, 5517.

57 G. Rostamikia and M. J. Janik, *Energy Environ. Sci.*, 2010, **3**, 1262.

58 S. A. Wasileski and M. J. Janik, *Phys. Chem. Chem. Phys.*, 2008, **10**, 3613.

59 K.-Y. Yeh and M. J. Janik, *J. Comput. Chem.*, 2011, **32**, 3399.

60 J.-L. Fattebert and F. Gygi, *Int. J. Quantum Chem.*, 2003, **93**, 139.

61 S. A. Petrosyan, A. A. Rigos and T. A. Arias, *J. Phys. Chem. B*, 2005, **109**, 15436.

62 Y.-H. Fang and Z.-P. Liu, *J. Am. Chem. Soc.*, 2010, **132**, 18214.

63 O. Andreussi, I. Dabo and N. Marzari, *J. Chem. Phys.*, 2012, **136**,.

64 K. Mathew, R. Sundararaman, K. Letchworth-Weaver, T. A. Arias and R. G. Hennig, *J. Chem. Phys.*, 2014, **140**, 084106.

65 C. J. Cramer and D. G. Truhlar, *Chem. Rev.*, 1999, **99**, 2161.

66 J. O. Bockris, A. K. N. Reddy and M. Gamboa-Aldeco, *Modern Electrochemistry 2A, Fundamental of Electrodics*, Kluwer Academic Publishers, New York, 2002.

67 *GoldBook, Standard Hydrogen electrode, http://goldbook.iupac.org/S05917.html*.

68 C. P. Kelly, C. J. Cramer and D. G. Truhlar, *J. Phys. Chem. B*, 2006, **110**, 16066.

69 Y. P. Zhang, C. H. Cheng, J. T. Kim, J. Stanojevic and E. E. Eyler, *Phys. Rev. Lett.*, 2004, **92**, 203003.

70 *If we use $2H^+ + 2e^- \rightarrow H_2$ to estimate the energy of H_2 at standard conditions, we need the energy of the solvated proton and the energy of the electrons. The hydration free energy of the proton is estimated to be about -11.5 eV[68]. Together with the electron potential of -4.44 V vs. vacuum, we get -31.88 eV, which is in good agreement with the "quantum chemical estimate" of 2*-13.6 eV (energy of a hydrogen atom) + -4.5 eV (binding energy of the hydrogen molecule[69])=-31.7 eV.*

71 *In the generalization of the CHE to an arbitrary reference couple (see ref 36) the severeness of this approximation is most clearly visible: the zero charge energy of a system always corresponds to the reversible potential of the reference redox couple. For example the zero charge energy of CO_2@Ni corresponds to 0 V, if we consider a hydrogenation, but to -2.7 V if we consider a reduction with sodium.*

72 S. A. Wasileski, M. T. M. Koper and M. J. Weaver, *J. Am. Chem. Soc.*, 2002, **124**, 2796.

73 A. Panchenko, M. T. M. Koper, T. E. Shubina, S. J. Mitchell and E. Ro-

duner, *J. Electrochem. Soc.*, 2004, **151**, A2016.

74 M. P. Hyman and J. W. Medlin, *J. Phys. Chem. B*, 2005, **109**, 6304.

75 S. A. Wasileski and M. J. Weaver, *J. Phys. Chem. B*, 2002, **106**, 4782.

76 J.-S. Filhol and M.-L. Doublet, *Catal. Today*, 2013, **202**, 87.

77 J.-S. Filhol and M.-L. Doublet, *J. Phys. Chem. C*, 2014, **118**, 19023.

78 Y.-H. Fang, G.-F. Wei and Z.-P. Liu, *J. Phys. Chem. C*, 2014, **118**, 3629.

79 R. C. Catapan, A. A. M. Oliveira, Y. Chen and D. G. Vlachos, *J. Phys. Chem. C*, 2012, **116**, 20281.

80 E. Westphal and J. R. Pliego, *J. Chem. Phys.*, 2005, **123**,.

81 M. Dusek, G. Chapuis, M. Meyer and V. Petricek, *Acta Crystallogr., Sect. B*, 2003, **59**, 337.

82 D. A. Reed and M. M. Olmstead, *Acta Crystallogr., Sect. B*, 1981, **37**, 938.

83 J. P. Perdew, K. Burke and M. Ernzerhof, *Phys. Rev. Lett.*, 1996, **77**, 3865.

84 P. E. Blochl, *Phys. Rev. B*, 1994, **50**, 17953.

85 G. Kresse and D. Joubert, *Phys. Rev. B*, 1999, **59**, 1758.

86 G. Kresse and J. Hafner, *Phys. Rev. B*, 1993, **47**, 558.

87 G. Kresse and J. Furthmuller, *Phys. Rev. B*, 1996, **54**, 11169.

88 D. Gunceler, K. Letchworth-Weaver, R. Sundararaman, K. A. Schwarz and T. A. Arias, *Modelling and Simulation in Materials Science and Engineering*, 2013, **21**, 074005.

89 K. Hara, A. Kudo and T. Sakata, *J. Electroanal. Chem.*, 1995, **391**, 141.

90 R. J. Lim, M. Xie, M. A. Sk, J.-M. Lee, A. Fisher, X. Wang and K. H. Lim, *Catal. Today*, 2014, **233**, 169.